DTIC FILE COPY

ARL-STRUC-TM-508

AR-005-610

AD-A218 051

DEPARTMENT OF DEFENCE

DEFENCE SCIENCE AND TECHNOLOGY ORGANISATION

AERONAUTICAL RESEARCH LABORATORY

MELBOURNE, VICTORIA

Aircraft Structures Technical Memorandum 508

STRESS CONCENTRATION FACTORS IN THE DESIGN OF LOADING FORKS (U)

by

D.C. Lombardo

Approved for Public Release

MAY 1989

90 02 ... 069

AR-005-610

DEPARTMENT OF DEFENCE
DEFENCE SCIENCE AND TECHNOLOGY ORGANISATION
AERONAUTICAL RESEARCH LABORATORY

Aircraft Structures Technical Memorandum 508

STRESS CONCENTRATION FACTORS IN THE DESIGN OF LOADING FORKS (U)

by

D.C. Lombardo

SUMMARY

Experimentally determined stress concentration factors arising at the edges of large pin holes in loading forks are examined in this report. The influence on these factors of fork size and pin type is also discussed. As well, the suitability of the Engineering Sciences Data Units (ESDU) data sheets in estimating stress concentration factors in large forks is shown.

DSTO ARL
MELBOURNE

POSTAL ADDRESS: Director, Aeronautical Research Laboratory,
P.O. Box 4331, Melbourne, Victoria, 3001, Australia

CONTENTS

1. INTRODUCTION

As part of the design of a fatigue test rig for an aircraft bulkhead, forks using large pins and capable of carrying up to 250 kips were required. The general configuration of the test rig and the forks under consideration are both shown in figure 1.

During testing, two different fork designs were used. One design was made from steel conforming to British Specification EN25 [1]* while the other was made from steel conforming to the American Iron and Steel Institute's H13 specification [2]. Each design consisted of two equal thickness lugs which transferred the applied load to the aircraft bulkhead. Two different fork designs (figure 2) were used because while the EN25 forks were available for use in the static strain surveys they were calculated to have an inadequate life under the fatigue loading. Hence, forks capable of carrying the fatigue loads were required and this led to the design of the H13 forks. The use of two different types of forks in this test provided the opportunity to place electric resistance strain gauges on both sets of forks to obtain experimental values of the stress concentration factors (SCFs). Additionally, these values could then be checked against the SCFs used in the fork design which were calculated from the Engineering Sciences Data Units (ESDU) engineering data sheets [3]. An interesting feature of these forks is that the gap between the fork lugs and the aircraft bulkhead is large (figure 2). This means that pin bending will be more significant than is usually the case where the gap is small.

Since the aircraft bulkhead being tested uses hollow pins in the fork/bulkhead attachment, both the EN25 and H13 forks were tested with hollow pins. Additionally, during commissioning of the rig, solid pins were used in the EN25 forks. Hence, it was possible to examine the changes in the SCF due to replacing a solid pin by a hollow pin.

2. STRAIN SURVEY

2.1 Strain gauge positioning

The gauges used in these tests were all TML uniaxial gauges, type FLA-6-23. The dimensions of these gauges are shown in figure 3(a). Note that these dimensions are large when compared to the expected strain gradients in the forks [4]. This means that some correction may need to be applied to the results in order to obtain peak strains.

2.1.1 EN25 forks - Four uniaxial strain gauges (labelled A, B, C & D) were placed on the fork shown in figure 1. The gauges were positioned as shown in figure 3(b) for the following reasons:

- gauge A was placed on the edge of the hole such that it would be at a point normal to the axis of the applied load.
- gauge B was at the edge of the hole on a line 35° from the normal because according to reference 3, for the given pin and hole geometries, the maximum SCF would occur at approximately this angle.
- gauges C and D were placed opposite A and B respectively because, due to pin bending, higher strains were expected on the inside of each lug.

* Numbers in brackets refer to the references at the end of the report

2.1.2 H13 forks - Five uniaxial strain gauges were placed on the fork shown in figure 1. These gauge positions (figure 3(c)) were chosen for the following reasons:

- gauges 3 and 4 correspond to gauges C and A respectively, thus allowing direct comparisons to be made.
- gauges 1 and 2 were placed on the opposite lug in order to determine whether any unequal load sharing was occurring.
- gauge 5 was used to provide a measure of the strain away from the hole.

2.2 Loading

All loading of the forks was done by installing them in the test rig. The EN25 forks were tested with both solid and hollow pins while the H13 forks only had hollow pins.

2.3 Experimental results

The strains were recorded manually using a Hottinger strain gauge readout box and a Kyowa switching box (Appendix 3). These readings are presented in tables 1 - 3. The data were then processed to produce the following:

– actual strains,	tables 4 - 6 and figures 4 - 5,
– strain ratios,	figure 6
– stresses,	tables 7 - 9,
– stress concentration factors,	tables 10 - 12 and figures 7 - 9.

Note that one of the measured values was not used since it was suspected that it had been misread. This value was for gauge 1 on the H13 fork at a load of 91 kips (see table 3).

3. ESDU STRESS CONCENTRATION FACTORS

The ESDU SCFs used in the design of both types of forks were calculated according to the method in [3]. The actual calculations are in Appendix 1 and the values are given below.

EN25 forks: SCF = 2.8
H13 forks: SCF = 4.14

4. DISCUSSION OF THE RESULTS

4.1 EN25 fork strains: hollow pin versus solid pin

The hollow pin was expected to bend more under load than the solid pin and the strain readings show that this is the case (figure 4). That is, $\epsilon_{hollow} < \epsilon_{solid}$ on the outside of the lugs and $\epsilon_{hollow} > \epsilon_{solid}$ on the inside. This is caused by pin bending transferring load away from the outside face of the lug towards the inside.

ie $\epsilon_{A_{hollow}} < \epsilon_{A_{solid}}$ outside face
$\epsilon_{B_{hollow}} < \epsilon_{B_{solid}}$ outside face
$\epsilon_{C_{hollow}} > \epsilon_{C_{solid}}$ inside face
$\epsilon_{D_{hollow}} > \epsilon_{D_{solid}}$ inside face.

The differences in the strains are quite dramatic. Table 13 shows that these range from a 75% decrease for the external gauges to a 28% increase for the internal gauges. This has implications for the SCFs in that a hollow pin will generate a larger maximum SCF. A comparison of figures 7 and 8 bears this out: the maximum hollow pin SCF is 2.28 whereas for the solid pin it is 1.92.

4.2 Load distribution in the H13 fork

As stated in section 2.1.2, gauges 1 and 2 were placed on the H13 fork in order to check for unequal load sharing between its two lugs. The expected results, if one lug was taking more load than the other, were either:

(i) $\epsilon_1 > \epsilon_4$ and $\epsilon_2 > \epsilon_3$
or (ii) $\epsilon_1 < \epsilon_4$ and $\epsilon_2 < \epsilon_3$.

However, figure 5 shows that this was not the case. The actual readings show $\epsilon_1 < \epsilon_4$ and $\epsilon_2 > \epsilon_3$. There are several possible solutions for this (figure 10), but in none of them is the existence of unequal load sharing required. Therefore the existence or otherwise of such loading could not be confirmed.

4.3 Hollow pin case - EN25 fork versus H13 fork

To properly compare the differences between the two designs, only the results from corresponding gauges should be used. That is, the results from gauges A and C (figure 3(b), EN25 fork) should be compared with those from gauges 4 and 3 (figure 3(c), H13 fork) respectively. The comments below are derived from comparisons between these four gauges.

4.3.1 Strain - As expected, due to their larger cross-sectional area, the H13 fork strains are less than those of the EN25 fork. Figure 6 consists of two graphs. The upper graph shows the the data for gauges A, C, 3 and 4 with linear regression applied to obtain straight line equations. These equations were then used to calculate the ratios ϵ_3/ϵ_C and ϵ_4/ϵ_A to produce the lower graph. This shows that, on average, ϵ_3 is 64% of ϵ_C and ϵ_4 is 81% of ϵ_A. (These values were calculated by neglecting the strain measurements below 25 kips.)

4.3.2 Stress concentration factors - A comparison of the maximum SCFs in the two forks shows that the H13 fork has a higher value than the EN25 fork. This may be understood by considering how SCFs are calculated

The SCF at a point is the ratio of the stress at that point to some nominal stress. Maximum SCFs are calculated by using peak stresses. In the case of the forks, the nominal stress is calculated by dividing the applied load on each lug by the area marked A_x in figure 3(b). Hence, the nominal stress is inversely proportional to changes in area at the same applied load. Since the H13 forks have an A_x almost twice that of the EN25 forks, then they have a nominal stress which is half that in the EN25 forks. In contrast, section 4.3.1 shows that the peak stresses in the H13 forks were more than half of those in the EN25 forks (actually, 64 - 81%). Therefore, the ratio of the peak stress to nominal stress (ie: the SCF) will be larger in the H13 forks. This implies that for a given hole size, the larger the width of the fork, the higher the SCF. Alternatively, the smaller the ratio of fork hole to fork width, the higher the SCF (as long as the ratio has a 'reasonable' value, ie: not close to 0.0 or 1.0).

4.4 ESDU versus experimental stress concentration factors

Four points may be made regarding the ESDU SCFs (section 3) and the experimental SCFs (figures 7 - 9 and tables 10 - 12). These are detailed below.

4.4.1 Load dependence - The results obtained for both fork types show that there is, initially, a strong dependence between the load and the experimental SCFs (figures 7 - 9). It is only at higher loads that the SCFs become reasonably independent of the applied load. In contrast, the ESDU values are constants with respect to the applied load. A possible explanation for this is that the applied load is not shared evenly between the two lugs on the fork as was assumed (see table 7). Given this, then the equation at the foot of table 7:

$$\sigma_{nom} = 0.5 * \text{forkload}/A_x$$

should be written as

$$\sigma_{nom_A} = k_A * \text{forkload}/A_x$$

and $\sigma_{nom_B} = k_B * \text{forkload}/A_x$

where: A represents one lug on the fork and B the other lug

$$k_B = 1 - k_A$$

$$k_A > 0.5$$

As higher loads are applied, k_A changes because clearances in the fork and fork/pin assemblies are being taken up which changes the load distribution between the two lugs. Therefore, by using σ_{nom} (which has k_A fixed as 0.5) to determine the SCF, an apparent dependence between load and SCF is seen. Eventually, at high enough loads, the value of k_A will reach a constant value, but not necessarily 0.5. Hence the value of the SCF will now become constant, but as long as k_A is greater than 0.5 then the measured SCF, which uses σ_{nom}, will be greater than the actual SCF. On lug B, the reverse is true and thus the real value of the SCF for the fork is somewhere between that calculated for lug A and that for lug B. Examination of the behaviour of gauges 2 and 3 in figure 9 shows this happening. Gauge 2 has a higher SCF than gauge 3 initially, but the two curves converge until they reach constant values very close to each other.

4.4.2 Effect of pin type - The results from the EN25 forks (section 4.1) show that the type of pin used affects the SCF because of differences in the amount of pin bending (and possibly distortion) between solid and hollow pins. Although the ESDU data sheet [3] recognises the effect of pin bending on the SCF, it only considers this from the point of view of fork thickness. The effect of pin geometry is not even mentioned which is a serious oversight. However, the information given can be used, albeit in a roundabout way, to estimate this effect.

4.4.3 Magnitude: ESDU versus Experimental - The ESDU SCFs are significantly greater than the experimental SCFs even though the effects of pin bending were not included in the calculations. For instance, taking the maximum value of the experimental SCFs for each fork (tables 10 - 12), then

		Experimental	ESDU
EN25	solid pin	1.92	2.8
	hollow pin	2.29	2.8
H13	Hollow pin	3.57	4.14

The ESDU values appear to be a conservative indication of the actual maximum SCFs, but is this true? As stated in section 2.1, the gauges used were large. Therefore, if a large strain gradient existed near the hole, the gauges would have output an average value of the strains across their width. Or perhaps the gauges were not exactly on the peak strain point which is possible if the strain gradient was very large. More testing is required before any certain conclusion can be reached, but an estimate of this gradient and hence the peak SCF can be obtained from [4].

The ESDU SCF is calculated for a joint with a solid pin so the above data provides a factor to allow for a hollow pin. This factor is the ratio of the experimental SCF derived for the EN25 forks/hollow pin case to the experimental SCF for the EN25 solid pin case (20%).

The calculations for these corrections are given in Appendix 2, but the results are shown below:

		Experimental	ESDU
EN25	solid pin	2.4	2.8
	hollow pin	2.8	3.4
H13	hollow pin	4.2	5.0

It can now be seen that the ESDU results are still greater than those calculated from the experiment. Therefore, for a solid pin case, the ESDU values are valid for fork design in that they are most likely conservative. For a hollow pin, the calculated value should be increased. For the hollow pins in this investigation, the increase is 20%. This factor of 20% may also be applied to pins with similar relative geometries to the ones used here or to pins with larger relative wall thicknesses. For pins with much smaller relative wall thicknesses, the factor to apply will be greater than 20%. However, the results from this report cannot be used to determine its magnitude.

4.4.4 Ratio of pin hole diameter to fork width - As stated in section 4.3.2, the smaller the ratio of hole size to fork width, the larger the SCF. Figures 1 and 2 in reference 3 indicate that this is the type of behaviour to expect and therefore the validity of the experimental results is supported.

5. CONCLUSIONS

(i) Engineering Sciences and Data Unit item 81006, although strictly for lugs may be used for forks provided that care is taken to allow for the effects of asymmetric loading and pin bending especially when hollow pins are used. The correction for bending should be to increase the calculated value by 20%.

(ii) If weight is not a major concern in the design of a pin joint, the use of a solid pin instead of a hollow pin is recommended since this reduces the maximum stress concentration factor in the fork.

REFERENCES

1. Woolman, J. and Mattram, R.A., " The mechanical and physical properties of the British Standard EN steels, Volume 2, EN21 - EN39", BS 970-1955, British Iron and Steel Association, 1966.
2. Metals Handbook, Volume 1, Properties and selection: Irons and Steels, 9th edition, American Society For Metals, 1978.
3. "Stress concentration factors, Axially loaded lugs with clearance fit pins", Engineering Sciences Data Item 81006, Amendment A, December 1982, Engineering Sciences Data Unit, London.
4. Theocaris, P. S., "The stress distribution in a strip loaded in tension by means of a central pin.", Trans. A.S.M.E. (Ser. E), J. Appl. Mech. **78**(1956), 85–90.

APPENDIX 1

CALCULATION OF ESDU STRESS CONCENTRATION FACTORS

Unless otherwise indicated, the calculations given below follow the procedure outlined in reference 3.

(i) EN25 FORK

Hole diameter, $d = 2.4976$ inches (max)
Pin diameter, $d_p = 2.4965$ inches (min)
Fork width, $w = 5$ inches
Lug thickness, $t = 1.07$ inches
Distance from fork end to hole centre, $a = 2.7$ inches

$\therefore$ $d/w = 0.50$, $a/w = 0.54$, $t/d = 0.43$

and e = pin-to-hole clearance as a percentage of d

$= 100 * (2.4976 - 2.4965)/2.4976$

$= 0.044\%$

Using figure 2 of [3] gives: $K'_{0.2} = 2.9$ and $K'_{100} = 3.9$
Using figure 3 of [3] gives: $\eta_e = -0.25$
where K'_m is the SCF for $e = m$
and η_e is a clearance correction factor

$\therefore$ Applying the formula:

$$K'_e = K'_{0.2} + \eta_e(K'_{100} - K'_{0.2})$$

gives

$$K'_e = 2.9 - 0.25(3.9 - 2.9) = 2.65$$

Now, introduce a factor to account for the gap between the two lugs on the fork and the connecting lug in the aircraft bulkhead. This gap was 0.12 inches on each side (figure 2).

$\therefore$ let g be the gap: $g = 0.12$ inches

Non-dimensionalise this with respect to the nominal pin diameter.

$\therefore$ $g' = g/d = 0.12/2.5 = 0.048$

To use this information, consider paragraph 3 of section 2.5 in [3]. Here the effect of a radius on the hole edge in the fork is discussed. This radius is given as $r = 0.18d$ (ie $r' = 0.18$, in non-dim. form) and the value of K'_e is 2.6 as against 2.07 for $r = 0$.

This gives $\Delta K'_e = (2.6 - 2.07)/2.07 = 0.26$

Assuming that (i) a radius r' is equivalent to having a gap, $g = r'$ and (ii) $\Delta K'_e$ is proportional to g' then :

$$\Delta K'_e = 0.26 * 0.048/0.18 = 0.07$$

Hence, SCF $= K'_e(1 + \Delta K'_e)$

$= 2.65(1 + 0.07)$

$= 2.8$

(ii) H13 FORK

Proceeding as for the EN25 forks:
d = 2.5 inches (max)
d_p= 2.4965 inches (min)
w = 8.0 inches
t = 1.0 inches
a = 3.6 inches

$\therefore \quad d/w = 0.31, \qquad a/w = 0.45, \qquad t/d = 0.43$
and $e = 100 * (2.4976 - 2.4965)/2.4976$
Using figure 2 of [3] gives: $K'_{0.2} = 3.95$ and $K'_{100} = 5.0$
Using figure 3 of [3] gives: $\eta_e = -0.08$

$$\therefore \qquad K'_e = 3.95 - 0.08(5.0 - 3.95) = 3.87$$

The H13 forks have the same gap, g and hence g', as the EN25 forks

$\therefore \quad \Delta K'_e = 0.07$

Hence, SCF = $3.87(1 + 0.07)$
$= 4.14$

APPENDIX 2

CORRECTIONS TO STRESS CONCENTRATION FACTORS

(i) EN25 FORK

Hole radius, $r = 1.249$ inches (max)
Fork width, $w = 5$ inches
Distance from hole centre to gauge C centre, $r_1 = 1.25 + 0.08 = 1.33$ inches

Let $\eta = r/(0.5w) = 0.5$
and $\eta_1 = r_1/(0.5w) = 0.532$

Using figure 2 of [4] gives: for $\eta = .5$, $\sigma_I/\sigma_m = 5$
Using figure 2 of [4] gives: for $\eta = .532$, $\sigma_I/\sigma_m = 4$

Hence, the SCF (σ_I/σ_m) increases by 25% when going from $\eta = .532$ to $\eta = .5$, ie, going from the centre of the gauge to the edge of the hole. Assuming that this factor can be applied to the SCFs measured in the test, then the solid pin SCF of 1.92 becomes $1.92 \times 1.25 = 2.4$ and the hollow pin SCF of 2.29 becomes $2.29 \times 1.25 = 2.9$.

(ii) H13 FORK

Proceeding as for the EN25 forks -

Hole radius, $r = 1.25$ inches (max)
Fork width, $w = 8$ inches
Distance from hole centre to gauge C centre, $r_1 = 1.25 + 0.08 = 1.33$ inches

$$\therefore \quad \eta = .312$$
$$\eta_1 = .332$$

Using figure 2 of [4] gives: for $\eta = .312$, $\sigma_I/\sigma_m = 5.2$
Using figure 2 of [4] gives: for $\eta = .332$, $\sigma_I/\sigma_m = 4.4$

Hence, the increase in the SCF is 17.6% when going from the centre of the gauge to the edge of the hole.

$\therefore$ Hollow pin SCF of 3.57 becomes $3.57 \times 1.176 = 4.2$

(iii) ESDU SCFs : the hollow pin cases

From the test, the SCFs for the EN25 lugs were determined to be 2.4 for the solid pin case and 2.9 for the hollow pin (see part (i) of this appendix). This represents an increase of:

$$\Delta = (2.9 - 2.4)/2.4 = 21\% \approx 20\%$$

Now, assume:

(i) that the ESDU SCF for the EN25 forks was correct for the case of a solid pin and
(ii) that Δ is a constant factor between the SCFs for the solid and hollow pin cases.

Therefore, ESDU SCF values corrected for a hollow pin may be obtained by:

$$\text{ESDU Hollow pin SCF} = (1 + \Delta) \times \text{ESDU Solid pin SCF}$$

	Solid pin SCF	Hollow pin SCF
EN25	2.8	3.4
H13	4.14	5.0

APPENDIX 3
TEST EQUIPMENT

The test equipment used consisted of:

(i) TML strain gauges, type FLA–6–23

(ii) Hottinger Baldwin Messtechnik, Type MK, readout box to obtain the strain gauge readings (serial no. J4085)

(iii) Kyowa Switching and Balancing box, Type SS-12R, to connect the strain gauges to the readout box (serial no. 4267)

TABLE 1: Strain Readings, EN25 Fork, Solid Pin

LOAD (kips)	A ($\mu\epsilon$)	B ($\mu\epsilon$)	C ($\mu\epsilon$)	D ($\mu\epsilon$)
0	25308	25032	25058	25640
26	25604	25298	25307	25790
51	25804	25431	25639	26030
63	25912	25507	25801	26148
77	26020	25584	25957	26265
90	26129	25664	26125	26373
103	26233	25743	26279	26488
114	26335	25826	26424	26608
0	25312	25042	25056	25646

TABLE 2: Strain Readings, EN25 Fork, Hollow Pin

LOAD (kips)	A ($\mu\epsilon$)	B ($\mu\epsilon$)	C ($\mu\epsilon$)	D ($\mu\epsilon$)
0	25392	25025	25061	25645
25	25537	25228	25349	25855
51	25676	25307	25723	26163
76	25844	25410	26097	26472
101	26020	25526	26472	26793
126	26188	25635	26851	27117
0		not	recorded	

TABLE 3: Strain Readings, H13 Fork, Hollow Pin

LOAD (kips)	1 ($\mu\epsilon$)	2 ($\mu\epsilon$)	3 ($\mu\epsilon$)	4 ($\mu\epsilon$)	5 ($\mu\epsilon$)
0	25623	25515	25035	25118	25036
23	25667	25764	25163	25254	25061
45	25741	25989	25382	25353	25064
68	25815	26210	25607	25445	25069
91	25994	26425	25834	25546	25066
110	25975	26636	26062	25647	25064
0	25625	25477	25041	25093	25024

TABLE 4: Actual Strains, EN25 Fork, Solid Pin

LOAD (kips)	ϵ_A ($\mu\epsilon$)	ϵ_B ($\mu\epsilon$)	ϵ_C ($\mu\epsilon$)	ϵ_D ($\mu\epsilon$)
0	0	0	0	0
26	296	266	249	150
51	496	399	581	390
63	604	475	743	508
77	712	554	899	625
90	821	632	1067	733
103	925	711	1221	848
114	1047	794	1366	968
0	4	10	-2	6

TABLE 5: Actual Strains, EN25 Fork, Hollow Pin

LOAD (kips)	ϵ_A ($\mu\epsilon$)	ϵ_B ($\mu\epsilon$)	ϵ_C ($\mu\epsilon$)	ϵ_D ($\mu\epsilon$)
0	0	0	0	0
25	145	203	288	210
51	284	282	662	518
76	452	385	1036	827
101	628	501	1411	1148
126	796	610	1790	1472

TABLE 6: Actual Strains, H13 Fork, Hollow Pin

LOAD (kips)	ϵ_1 ($\mu\epsilon$)	ϵ_2 ($\mu\epsilon$)	ϵ_3 ($\mu\epsilon$)	ϵ_4 ($\mu\epsilon$)	ϵ_5 ($\mu\epsilon$)
0	0	0	0	0	0
23	44	249	128	136	25
45	118	474	347	235	28
68	192	695	572	327	33
91	-	910	799	428	30
110	352	1121	1027	529	28
0	2	-38	6	-25	-12

TABLE 7: Stresses, EN25 Fork, Solid Pin

LOAD (kips)	σnom (ksi)	σA (ksi)	σB (ksi)	σC (ksi)	σD (ksi)
0	0.0	0.0	0.0	0.0	0.0
26	4.8	8.9	8.1	7.6	4.5
51	9.5	14.9	12.0	17.4	11.7
63	12.0	18.1	14.3	22.3	15.2
77	14.4	21.4	16.6	27.0	18.8
90	16.8	24.6	19.0	32.0	22.0
103	19.2	27.8	21.3	36.6	25.4
114	21.3	31.4	23.8	41.0	29.0

NOTE: $\sigma nom = \dfrac{0.5 \text{ x Fork Load (kips)}}{\text{Ax (in}^2\text{) (see fig 3(a))}}$

$= \dfrac{0.5 \text{ x Fork Load}}{2.68}$

: σi = Esteel x ϵi, where i = A, B, C, D ,E
= $0.030\epsilon i$, for ϵ in micro-strain and σ in ksi

TABLE 8: Stresses, EN25 Fork, Hollow Pin

LOAD (kips)	σnom (ksi)	σA (ksi)	σB (ksi)	σC (ksi)	σD (ksi)
0	0.0	0.0	0.0	0.0	0.0
25	4.7	4.4	6.1	8.6	6.3
51	9.4	8.5	8.5	19.9	15.5
76	14.1	13.6	11.6	31.1	24.8
101	18.8	18.8	15.0	42.3	34.4
126	23.5	23.9	18.3	53.7	44.2

See note for Table 7

TABLE 9: Stresses, H13 Fork, Hollow Pin

LOAD (kips)	σnom (ksi)	σ1 (ksi)	σ2 (ksi)	σ3 (ksi)	σ4 (ksi)	σ5 (ksi)
0	0.0	0.0	0.0	0.0	0.0	0.0
23	2.1	1.3	7.5	3.8	4.1	0.8
45	4.1	3.5	14.2	10.4	7.1	0.8
68	6.2	5.8	20.9	17.2	9.8	1.0
91	-	11.1	27.3	24.0	12.8	0.9
110	10.3	10.6	33.6	30.8	15.6	0.8

NOTE: Calculation of stresses is as per the note for Table 7 except that Ax is 5.51 in^2.

TABLE 10: Stress Concentration Factors
EN25 Fork, Solid Pin

LOAD (kips)	SCFA	SCFB	SCFC	SCFD
0	-	-	-	-
26	1.85	1.66	1.56	0.94
51	1.57	1.26	1.83	1.23
63	1.51	1.19	1.86	1.27
77	1.49	1.15	1.88	1.31
90	1.46	1.13	1.90	1.31
103	1.45	1.11	1.91	1.32
114	1.47	1.12	1.92	1.36

Note: $SCFi = \frac{\text{Fork stress at gauge } i}{\text{Nominal stress}}$, i = A, B, C, D, E

TABLE 11: Stress Concentration Factors
EN25 Fork, Hollow Pin

LOAD (kips)	SCFA	SCFB	SCFC	SCFD
0	-	-	-	-
25	0.93	1.30	1.84	1.34
51	0.90	0.90	2.11	1.65
76	0.96	0.82	2.21	1.76
101	1.00	0.80	2.25	1.83
126	1.02	0.78	2.29	1.88

See note for Table 10

TABLE 12: Stress Concentration Factors
H13 Fork, Hollow Pin

LOAD (kips)	SCF1	SCF2	SCF3	SCF4	SCF5
0	-	-	-	-	-
23	0.62	3.57	1.81	1.95	0.38
45	0.85	3.46	2.53	1.73	0.20
68	0.94	3.37	2.77	1.58	0.16
91	-	3.33	2.93	1.56	0.11
110	1.03	3.26	3.00	1.51	0.08

See note for Table 10

TABLE 13: Strains - Hollow Pin vs Solid Pin, EN25 Fork

	Load ≈ 50 kips		Load ≈ 75 kips	
	Strain ($\mu\epsilon$)	ϵdiff (%)	Strain ($\mu\epsilon$)	ϵdiff (%)
A - Hollow	284	-74.6%	452	-57.5%
- Solid	496		712	
B - Hollow	282	-41.5%	385	-43.9%
- Solid	399		554	
C - Hollow	662	12.2%	1036	13.2%
- Solid	581		899	
D - Hollow	518	24.7%	827	24.4%
- Solid	390		625	

	Load ≈ 100 kips		Load = 114 kips	
	Strain ($\mu\epsilon$)	ϵdiff (%)	Strain ($\mu\epsilon$)	ϵdiff (%)
A - Hollow	628	-47.3%	720	-45.4%
- Solid	925		1047	
B - Hollow	501	-41.9%	565	-40.5%
- Solid	711		794	
C - Hollow	1411	13.5%	1625	15.9%
- Solid	1221		1366	
D - Hollow	1148	26.1%	1340	27.8%
- Solid	848		968	

NOTE: ϵdiff = 100 (ϵHollow - ϵSolid) / ϵHollow

: The hollow pin strain values at 114 kips load are interpolated from the values at 101 and 126 kips.

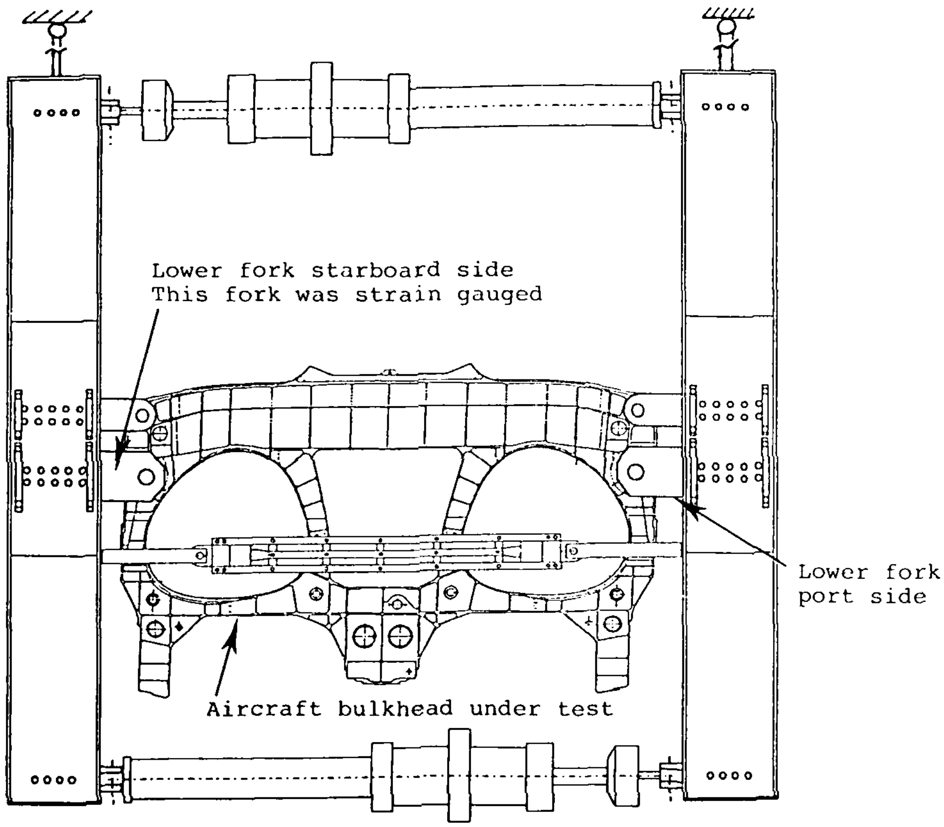

FIG 1: GENERAL CONFIGURATION OF THE TEST RIG AND TEST ARTICLE

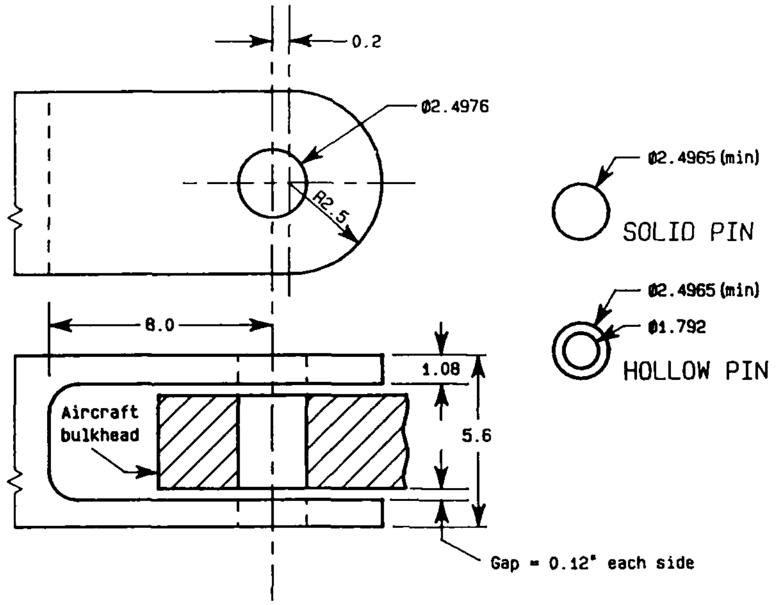

ALL DIMENSIONS IN INCHES

FIG 2(a). EN25 FORK AND THE SOLID AND HOLLOW PINS.
(ONLY THE FRONT END OF THE FORK HAS BEEN SHOWN.)

ALL DIMENSIONS IN INCHES

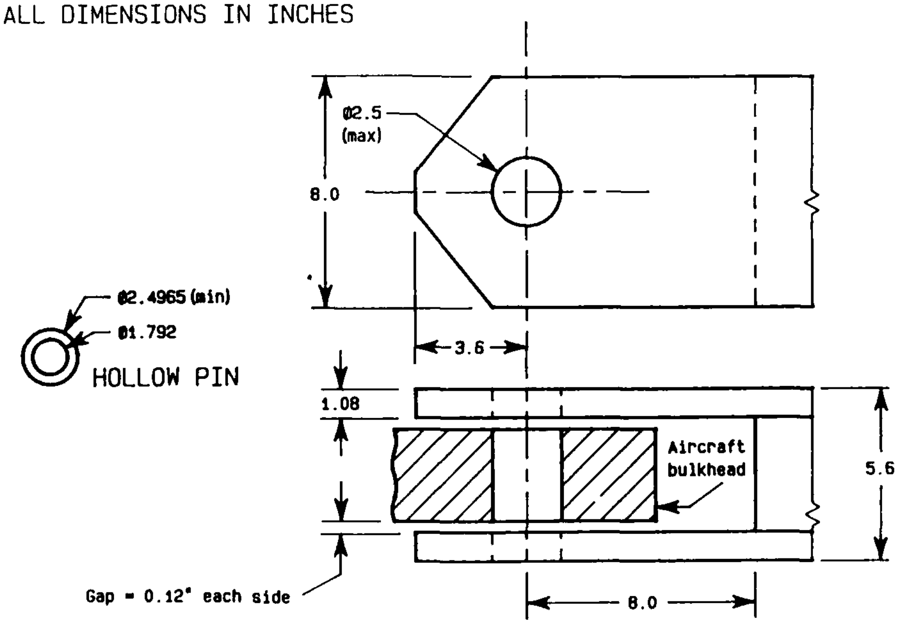

FIG 2(b). H13 FORK AND THE HOLLOW PIN.
(ONLY THE FRONT END OF THE FORK HAS BEEN SHOWN.)

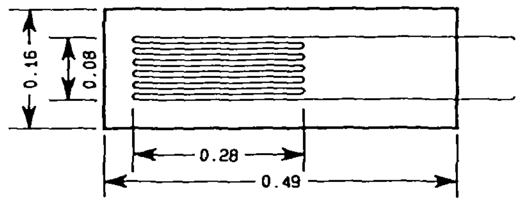

FIG 3(a). STRAIN GAUGE DIMENSIONS IN INCHES.

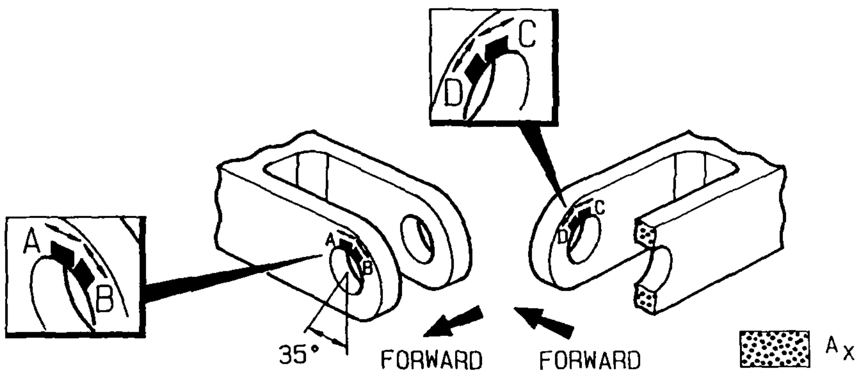

DOUBLE-HEADED ARROWS INDICATE GAUGE DIRECTIONS.

FIG 3(b). FRONT AND REAR VIEWS OF THE EN25 FORK SHOWING THE STRAIN GAUGE POSITIONS (A_X IS REFERRED TO IN SECTION 4. 3. 2.).

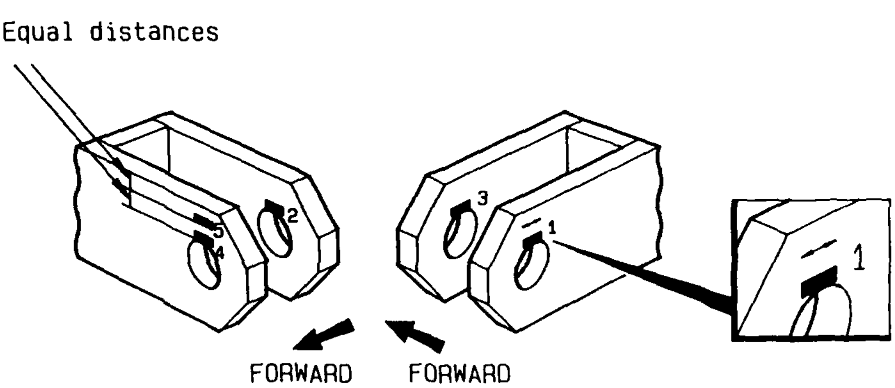

FIG 3(c). FRONT AND REAR VIEWS OF THE H13 FORK SHOWING THE GAUGE POSITIONS ALL GAUGE DIRECTIONS ARE THE SAME AS INDICATED FOR GAUGE 1.

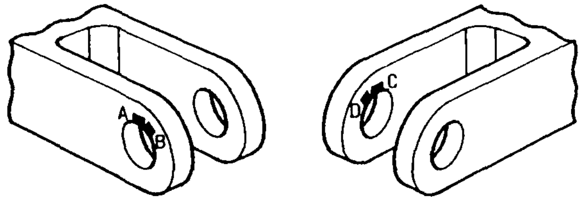

Gauge locations

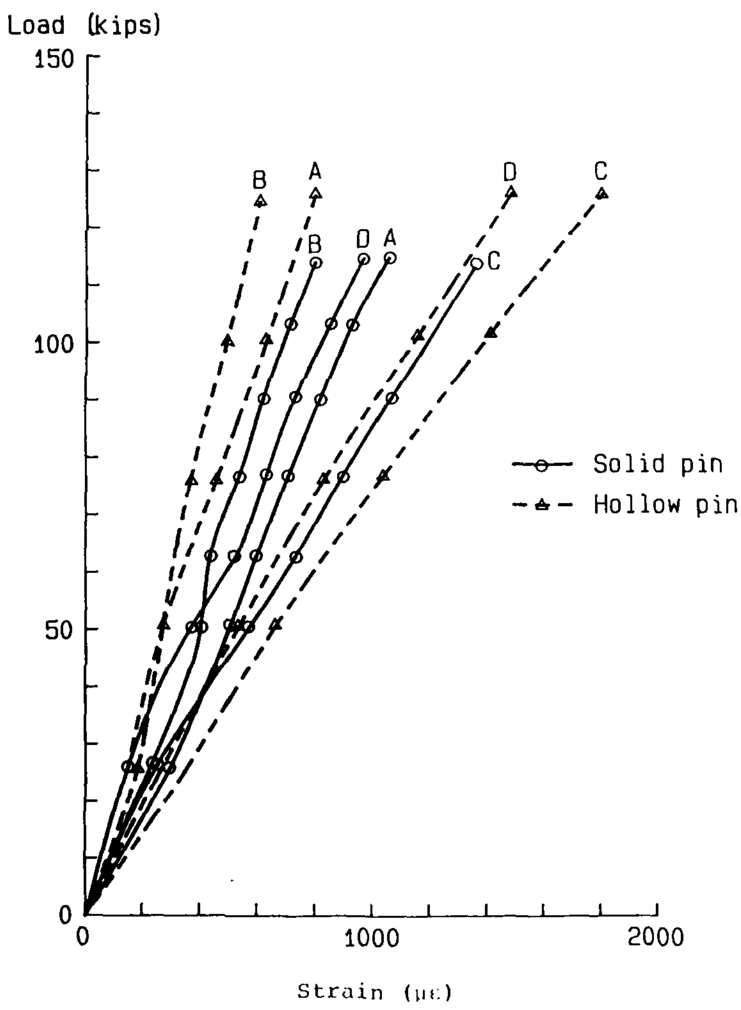

FIG 4. EN25 FORK STRAINS.

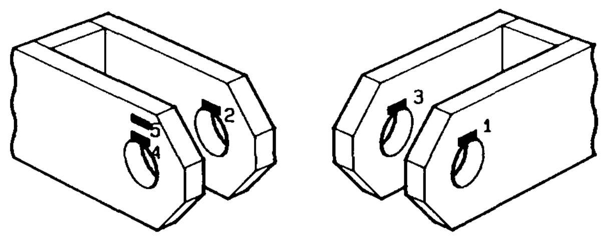

Gauge locations

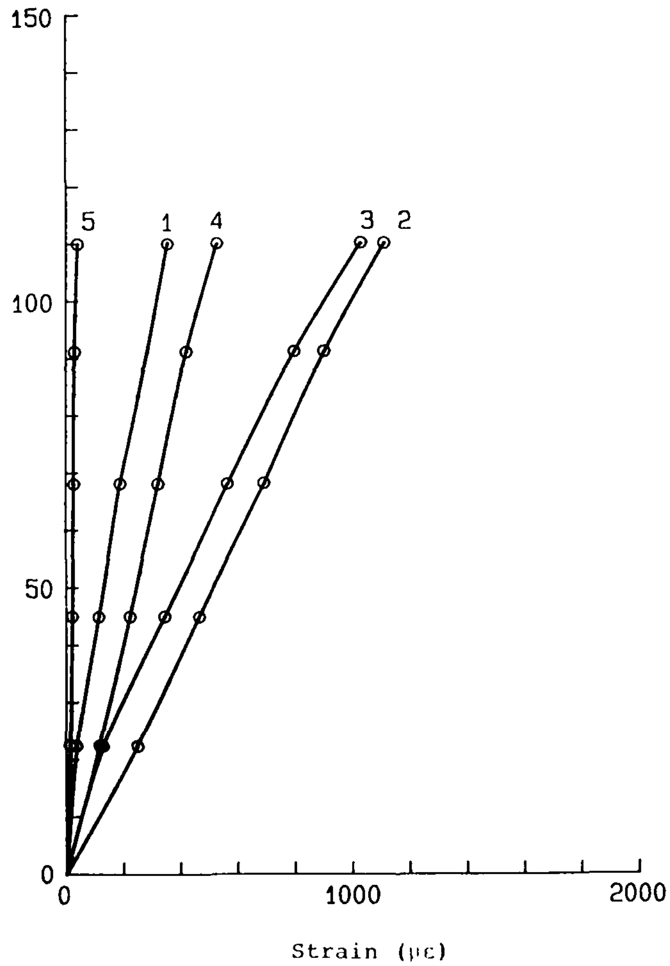

FIG 5. H13 FORK STRAINS.

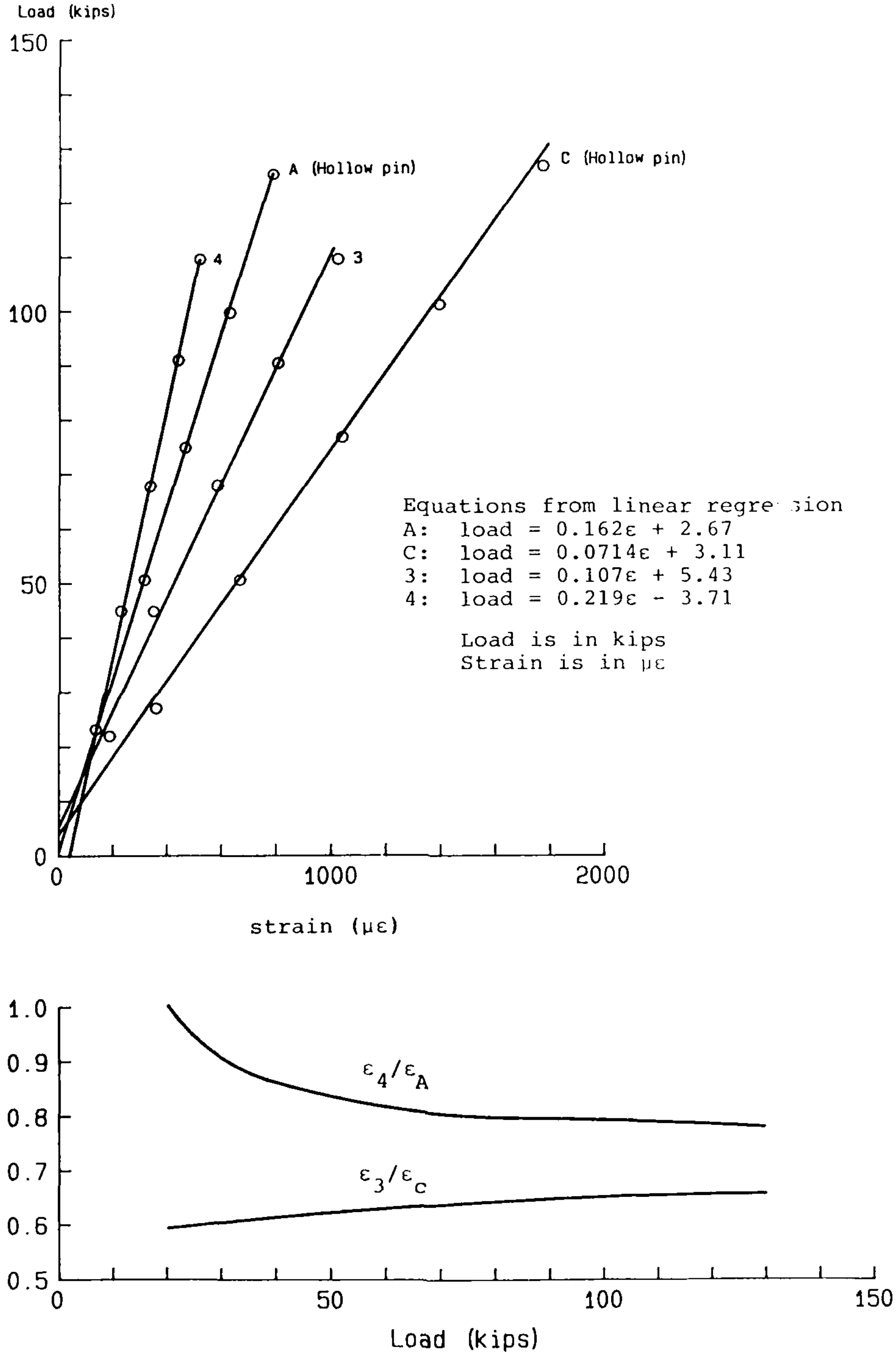

FIG 6. COMPARISION OF PEAK STRAINS IN THE H13 FORK
AND THE EN25 FORK WITH HOLLOW PINS.

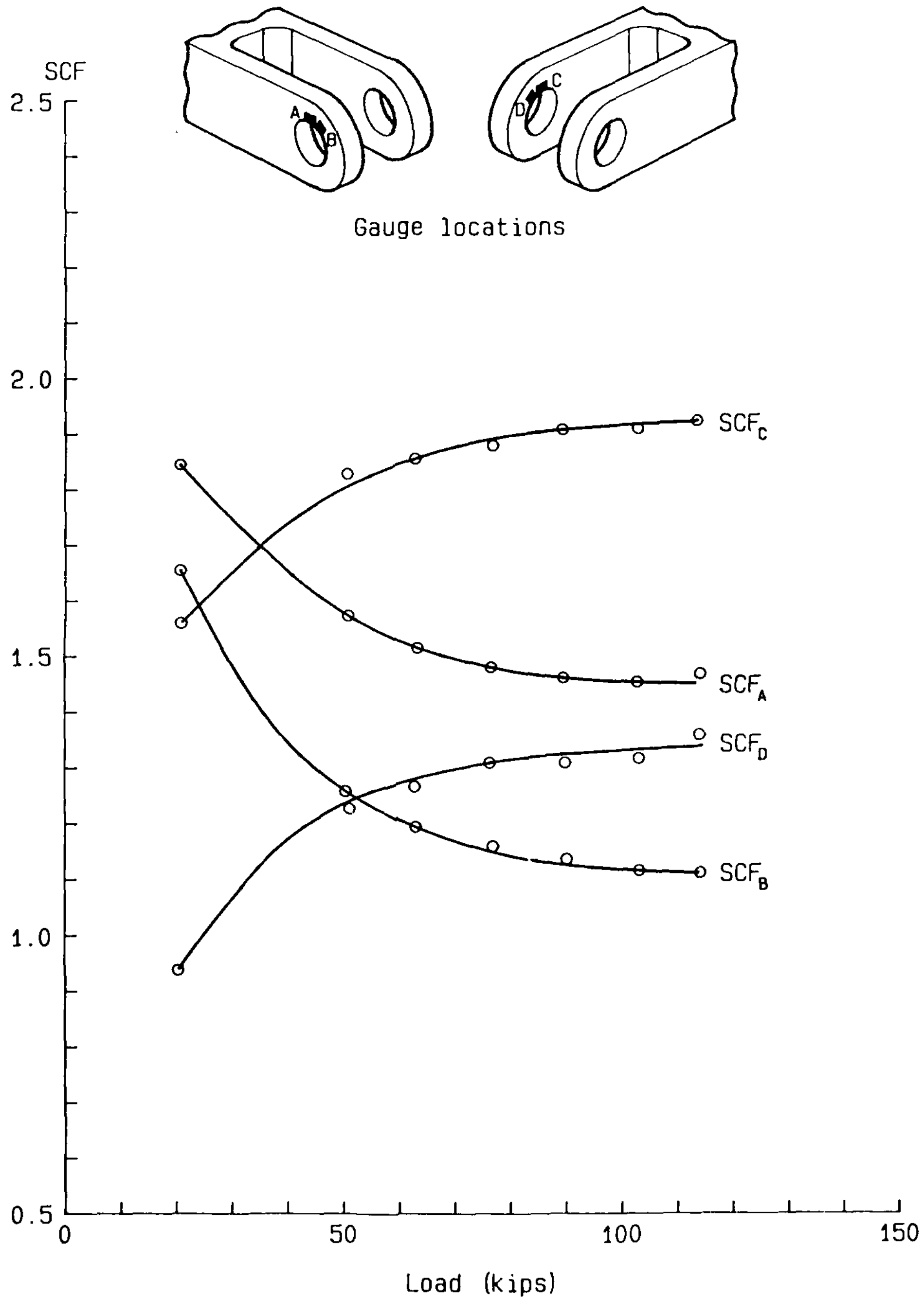

FIG 7. STRESS CONCENTRATION FACTORS FOR THE EN25 FORK WITH A SOLID PIN.

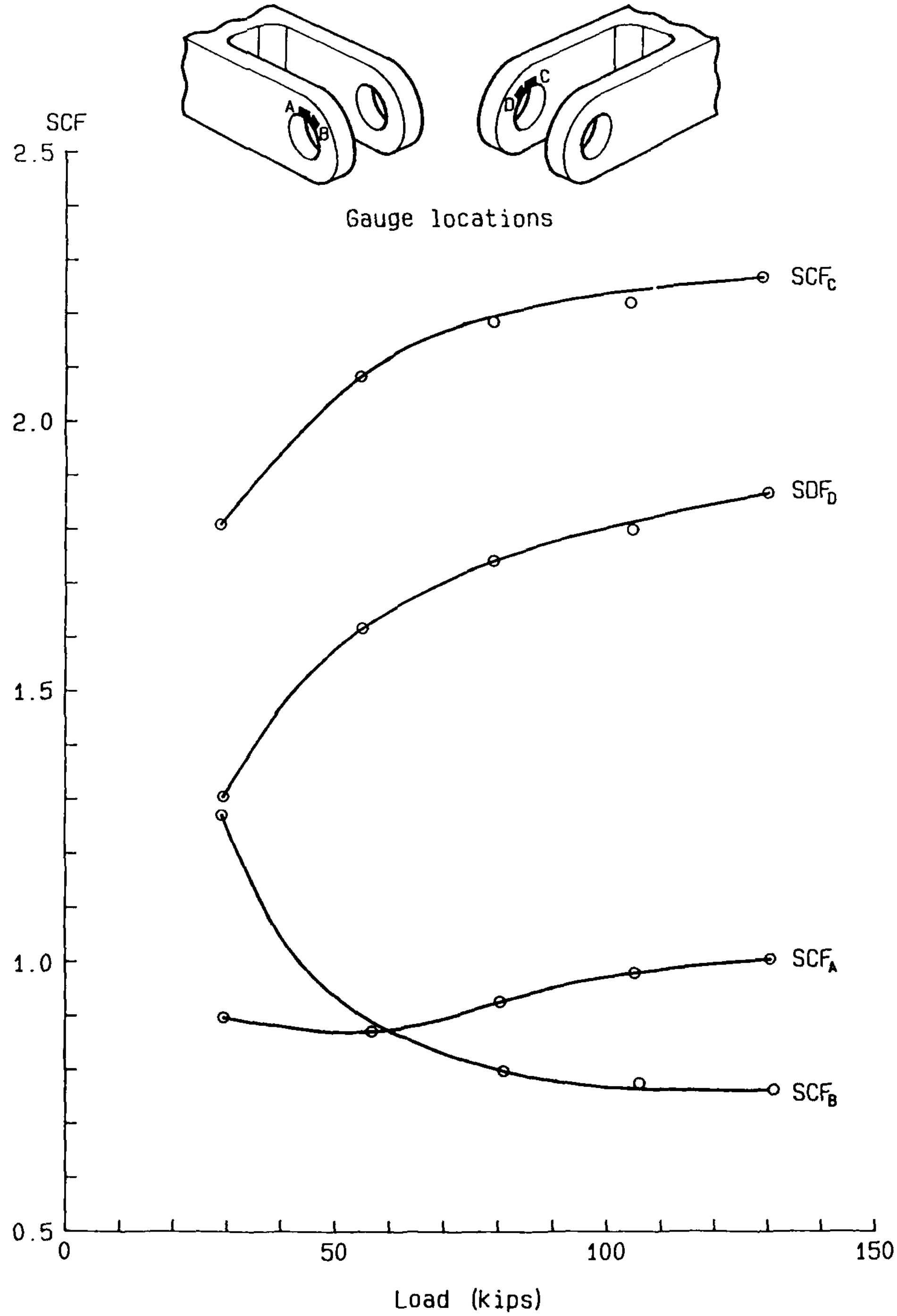

FIG 8. STESS CONCENTRATION FACTORS FOR THE EN25 FORK WITH A HOLLOW PIN.

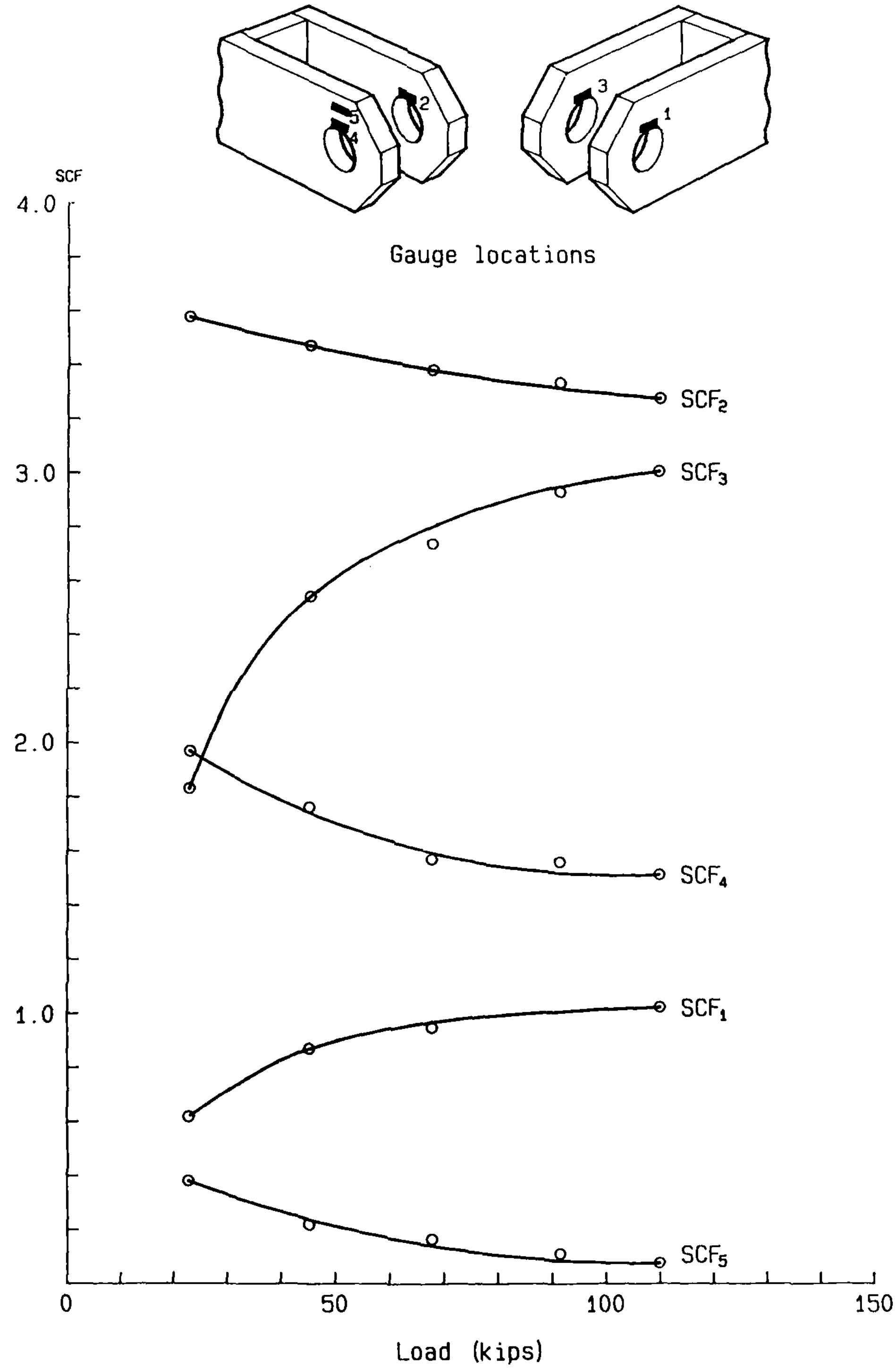

FIG 9. STRESS CONCENTRATION FACTORS FOR THE H13 FORK.

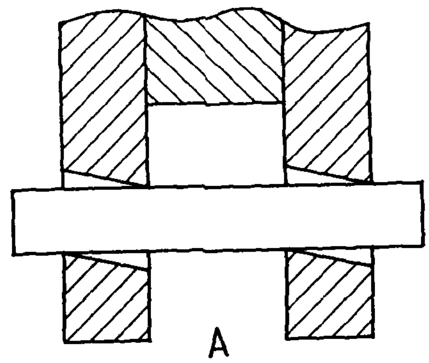

THE HOLES ARE NOT PERPENDICULAR TO THE SURFACE

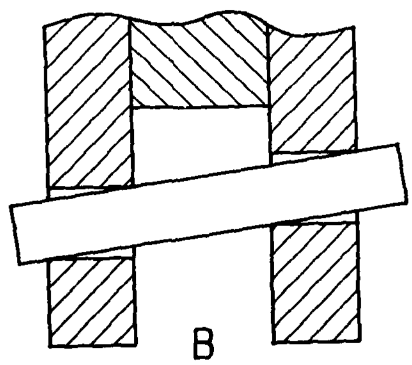

THE TWO HOLES ARE NOT IN LINE WITH EACH OTHER

FIG 10. TWO POSSIBLE SOLUTIONS TO THE PROBLEM OF SECTION 4.2.

DISTRIBUTION

AUSTRALIA

Department of Defence

Defence Central
Chief Defence Scientist
FAS Science Corporate Management (shared copy)
FAS Science Policy (shared copy)
Director, Departmental Publications
Counsellor, Defence Science, London (Doc Data Sheet Only)
Counsellor, Defence Science, Washington (Doc Data Sheet Only)
S.A. to Thailand MRD (Doc Data Sheet Only)
S.A. to the DRC (Kuala Lumpur) (Doc Data Sheet Only)
OIC TRS, Defence Central Library
Document Exchange Centre, DISB (18 copies)
Joint Intelligence Organisation
Librarian H Block, Victoria Barracks, Melbourne
Director General - Army Development (NSO) (4 copies)

Aeronautical Research Laboratory
Director
Library
Divisional File - Aircraft Structures
Author: D.C. Lombardo
R. Parker
G. Revill
T. Van Blaricum
G. Jost

Materials Research Laboratory
Director/Library

Defence Science & Technology Organisation - Salisbury
Library

Navy Office
Navy Scientific Adviser (3 copies Doc Data sheet)
Director of Naval Ship Design

Army Office
Scientific Adviser - Army (Doc Data sheet only)
Engineering Development Establishment, Library

Air Force Office
Air Force Scientific Adviser (Doc Data sheet only)
Aircraft Research and Development Unit
Library
Engineering Division Library

Statutory and State Authorities and Industry
Aero-Space Technologies Australia, Manager/Librarian (2 copies)
Hawker de Havilland Aust Pty Ltd, Victoria, Library
Hawker de Havilland Aust Pty Ltd, Bankstown, Library

Universities and Colleges
NSW
Library, Australian Defence Force Academy

SPARES (5 copies)
TOTAL (51 copies)

AL 149

DEPARTMENT OF DEFENCE

DOCUMENT CONTROL DATA

PAGE CLASSIFICATION
UNCLASSIFIED

PRIVACY MARKING

1a. AR NUMBER	1b. ESTABLISHMENT NUMBER	2. DOCUMENT DATE	3. TASK NUMBER
AR-005-610	ARL-STRUC-TM-508	MAY 1989	DST 85/138

4. TITLE
STRESS CONCENTRATION FACTORS IN THE DESIGN OF LOADING FORKS

5. SECURITY CLASSIFICATION (PLACE APPROPRIATE CLASSIFICATION IN BOX(S) IE. SECRET (S), CONF.(C) RESTRICTED (R), UNCLASSIFIED (U)).

DOCUMENT	TITLE	ABSTRACT
U	U	U

6. NO. PAGES
26

7. NO. REFS.
4

8. AUTHOR(S)
D.C. LOMBARDO

9. DOWNGRADING/DELIMITING INSTRUCTIONS
Not applicable

10. CORPORATE AUTHOR AND ADDRESS

AERONAUTICAL RESEARCH LABORATORY
P.O. BOX 4331, MELBOURNE VIC 3001

11. OFFICE/POSITION RESPONSIBLE FOR:

SPONSOR DSTO
SECURITY –
DOWNGRADING –
APPROVAL CSTD

12. SECONDARY DISTRIBUTION (OF THIS DOCUMENT) Approved for public release.

OVERSEAS ENQUIRIES OUTSIDE STATED LIMITATIONS SHOULD BE REFERRED THROUGH ASDIS, DEFENCE INFORMATION SERVICES BRANCH, DEPARTMENT OF DEFENCE, CAMPBELL PARK, CANBERRA, ACT 2601

13a. THIS DOCUMENT MAY BE ANNOUNCED IN CATALOGUES AND AWARENESS SERVICES AVAILABLE TO....
No limitations.

13b. CITATION FOR OTHER PURPOSES (IE. CASUAL ANNOUNCEMENT) MAY BE [X] UNRESTRICTED OR [ ] AS FOR 13a.

14. DESCRIPTORS

Fatigue tests	Test stands
Forks	Stress concentration
Loading	Pinholes

15. DRDA SUBJECT CATEGORIES
0051f
0094J
0041G

16. ABSTRACT
Experimentally determined stress concentration factors arising at the edges of large pin holes in loading forks are examined in this report. The influence on these factors of fork size and pin type is also discussed. As well, the suitability of the Engineering Sciences Data Units (ESDU) data sheets in estimating stress concentration factors in large forks is shown.

PAGE CLASSIFICATION
UNCLASSIFIED

PRIVACY MARKING

THIS PAGE IS TO BE USED TO RECORD INFORMATION WHICH IS REQUIRED BY THE ESTABLISHMENT FOR ITS OWN USE BUT WHICH WILL NOT BE ADDED TO THE DISTIS DATA UNLESS SPECIFICALLY REQUESTED.

16. ABSTRACT (CONT.)		
17. IMPRINT AERONAUTICAL RESEARCH LABORATORY, MELBOURNE		
18. DOCUMENT SERIES AND NUMBER Aircraft Structures Technical Memorandum 508	19. COST CODE 241606	20. TYPE OF REPORT AND PERIOD COVERED
21. COMPUTER PROGRAMS USED		
22. ESTABLISHMENT FILE REF.(S)		
23. ADDITIONAL INFORMATION (AS REQUIRED)		